Enzyme Multilayer-Modified Porous Membranes as Biocatalysts

Aimin Yu, Zhijian Liang, and Frank Caruso*

Centre for Nanoscience and Nanotechnology, Department of Chemical and Biomolecular Engineering, The University of Melbourne, Victoria 3010, Australia

Received August 13, 2004. Revised Manuscript Received September 28, 2004

Porous polycarbonate (PC) membranes with pore diameters of either 400 or 100 nm were used as supports for the layer-by-layer deposition of peroxidase−poly(sodium 4-styrenesulfonate) complexes [(POD−PSS)$_c$] and oppositely charged poly(allylamine hydrochloride) (PAH) to prepare high-surface-area thin films for biocatalysis. Formation of the multilayer films was verified by scanning electron microscopy and transmission electron microscopy following dissolution of the porous PC template to generate POD/polyelectrolyte (PE) tubes. An average thickness of ∼5 nm was calculated for each (POD−PSS)$_c$/PAH bilayer, as determined from microscopy images. The activity of the POD/PE multilayer films was found to be dependent on the amount of enzyme in the film (which is determined by the number of (POD−PSS)$_c$ layers deposited) and the total membrane surface area. Films deposited on the PC membranes with 100-nm-diameter pores showed maximum bioactivity at five (POD−PSS)$_c$ layers. Beyond this layer number the total membrane activity decreased sharply, which is attributed to membrane pore blockage. Films deposited on PC membranes with pore diameters of 400 nm showed regularly increasing bioactivity up to seven (POD−PSS)$_c$ layers, with a plateau in activity observed thereafter. Activity enhancements of up to almost an order of magnitude larger were observed for the enzyme films deposited on the PC membranes (e.g., 100-nm pore diameter membranes with 4% porosity), compared with identical films formed on nonporous supports (e.g., quartz slides) with the same geometrical area. The reported method for the preparation of membrane-supported biocatalysts provides a viable approach for the generation of high-enzyme-content thin films with tailored bioactivity.

Introduction

The construction of protein-based thin films has long attracted widespread interest, largely because of their relevance to biotechnology. For example, protein films are routinely employed in bioseparations, immunoassays, diagnostics, localization, and catalysis.[1−5] Protein thin films are commonly prepared by physical adsorption, solvent casting, covalent binding, electropolymerization, Langmuir−Blodgett deposition, and sol−gel methods.[1] Recently, interest has also focused on the preparation of multilayer protein films. Such multilayer architectures can be engineered to contain a high density of biomolecules, which can lead to enhanced sensitivities for the detection of biomolecular species. Biospecific interactions, such as biotin−streptavidin binding, have been exploited to fabricate a wide array of protein multilayer architectures.[6−8] More recently, the layer-by-layer (LbL) method[9,10] has been utilized to fabricate protein multilayers via the sequential assembly of various proteins and oppositely charged polyelectrolytes (PEs).[11−17] The utility of LbL processed protein multilayers has been demonstrated in the areas of biocatalysis[12−14]and immunosensing.[15] However, in the biocatalysis field, one key issue pertaining to LbL enzyme multilayered films is that substrate diffusion becomes progressively dominant as the film thickness increases, hence directly limiting the activity and performance of the films.[1,12,19,20] The influence of such substrate diffusion effects in enzyme multilayers can be counterbalanced by employing high-surface-area supports for film formation. For example, we recently reported the preparation

* To whom correspondence should be addressed. Fax: +61 3 8344 4153. E-mail: fcaruso@unimelb.edu.au.

(1) Lvov, Y., Möhwald, H., Eds. *Protein Architecture: Interfacing Molecular Assemblies and Immobilization Biotechnology*; Marcel Dekker: New York, 2000.
(2) Horbett, T. A., Brash, J. L., Eds. *Proteins at Interfaces: Fundamentals and Applications*; ACS Symposium Series 602; American Chemical Society: Washington, DC, 1995.
(3) Catty, D., Raykundalla, C., Eds. *Antibodies: A Practical Approach*; IRL Press: Oxford, 1989; Vol. II, p 97.
(4) Turner, A. P. F., Karube, I., Wilson, G. S., Eds. *Biosensors: Fundamentals and Applications*; Oxford University Press: Oxford, 1987.
(5) Guesdon, J. L.; Avrameas, S. In *Applied Biochemistry and Bioengineering*; Wingard, L. B., Katchalski-Katzir, E., Goldstein, L., Eds.; Academic Press: New York, 1981; Vol. 3, p 207.
(6) Anzai, J.; Takeshita, H.; Hoshi, T.; Osa, T. *Chem. Pharm. Bull.* **1995**, *43*, 520.
(7) Cassier, T.; Lowack, K.; Decher, G. *Supramol. Sci.* **1998**, *5*, 309.
(8) Edmiston, P. L.; Saavedra, S. S. *J. Am. Chem. Soc.* **1998**, *120*, 1665.
(9) Decher, G.; Hong, J. D. *Ber. Bunsen-Ges* **1991**, *95*, 1430.
(10) Decher, G. *Science* **1997**, *277*, 1232.
(11) Lvov, Y.; Ariga, K.; Ichinose, I.; Kunitake, T. *J. Am. Chem. Soc.* **1995**, *117*, 6117.
(12) Onda, M.; Ariga, K.; Kunitake, T. *J. Biosci. Bioeng.* **1999**, *87*, 69.
(13) Onda, M.; Lvov, Y.; Ariga, K.; Kunitake, T. *Biotechnol. Bioeng.* **1996**, *51*, 163.
(14) Onda, M.; Lvov, Y.; Ariga, K.; Kunitake, T. *J. Ferm. Bioeng.* **1996**, *82*, 502
(15) Caruso, F.; Niikura, K.; Furlong, D. N.; Okahata, Y. *Langmuir* **1997**, *13*, 3427.
(16) Caruso, F.; Furlong, D. N.; Ariga, K.; Ichinose, I.; Kunitake, T. *Langmuir* **1998**, *14*, 4559.
(17) Lvov, Y. M.; Sukhorukov, G. B. *Biol. Membr.* **1997**, *14*, 229.
(18) Caruso, F.; Fiedler, H.; Haage, K. *Colloids Surf. A* **2000**, *169*, 287.
(19) Schüler, C.; Caruso, F. *Macromol. Rapid Commun.* **2000**, *21*, 750.
(20) Caruso, F.; Schüler, C. *Langmuir* **2000**, *16*, 9595.

10.1021/cm048659h CCC: $30.25
Published on Web 12/01/2004

of colloids with enzyme/PE multilayer shells.[18−21] The inherently high surface area of colloidal particles makes them especially useful for exploitation as enzyme carriers. We demonstrated that these enzyme/PE multilayer-coated particles are efficient colloidal enzymatic biocatalysts. Additionally, the particles can be prepared with tailored catalytic activities (depending on the number of enzyme layers deposited) and with multiple catalytic functions.[20] As part of our efforts focusing on the preparation of high-surface-area enzyme thin films, we have recently also reported the use of macroporous supports (both inorganic and polymer frameworks) for enzyme immobilization.[22,23] For macroporous zeolitic supports, the enzyme adsorbed amounts and activities show an approximate linear correlation with membrane thickness,[22] while enzyme-loaded porous polymer films can be readily utilized for potentiometric analyte detection.[23] For both systems, the film efficiency or sensing enhancement was significantly higher (approximately an order of magnitude) than that of corresponding films with closed macropores (i.e., nonporous films).

Herein, we examine the use of porous membrane supports for the preparation of LbL enzyme/PE multilayers on polycarbonate (PC) membranes with varying pore sizes. The formation of multilayers of different materials on porous membranes via the LBL approach has recently been reported.[24−26] Following dissolution of the membrane template, nanotubes comprised of polyelectrolytes,[24,25] polyelectrolyte/nanoparticle,[24] and α,ω-diorganophosphonate/Zr[26] have been prepared. In the current work, we deposit enzyme complexes (peroxidase−poly(sodium 4-styrenesulfonate), (POD-PSS)$_c$] in alternation with oppositely charged poly(allylamine hydrochloride) (PAH) on the porous PC membranes to obtain membrane-supported enzyme multilayers for biocatalysis investigations. The effect of membrane pore size, porosity, and film thickness on membrane bioactivity is examined. This approach enables the preparation of membrane-immobilized enzyme biocatalysts with tailored bioactivity.

Experimental Section

Materials. PC membranes (46-mm diameter) with pore diameters of 100 or 400 (±20%) nm, a pore depth of 10 μm, and porosities of 4 and 13%, respectively, were obtained from Millipore.[27] Poly(ethyleneimine) (PEI, M_w 25 000), PAH (M_w 70 000), PSS (M_w 70 000), POD, *o*-dianisidine, and hydrogen peroxide (H_2O_2) were purchased from Sigma-Aldrich. All chemicals were used as received, except PSS, which was dialyzed against Milli-Q water (M_w cutoff 14 kDa) and lyophilized prior to use. Phosphate buffer (PB) solutions of different pHs were prepared from 0.05 M NaH_2PO_4, Na_2HPO_4, and NaOH. Aqueous solutions containing (POD−PSS)$_c$ were prepared by adding POD and PSS to a vial and then diluting with 0.05 M pH 5.0 PB. The final concentrations of POD and PSS in the solutions were 1 and 2 mg mL^{-1}, respectively. Under the conditions used, the (POD−PSS)$_c$ are negatively charged, as assessed by ζ-potential measurements.[20] PE (PEI, PSS, and PAH) solutions of 1 mg mL^{-1} in water containing 0.5 M NaCl were used for depositing individual PE layers. The water used in all experiments was prepared in a Milli-Q system and had a resistivity higher than 18.2 MΩ cm.

Multilayer Film Formation on PC Membranes. Positively charged PEI was first adsorbed by immersing the membranes into a PEI solution, immediately sonicating for 2 min, and allowing 60 min for adsorption. The PEI-modified membrane was then rinsed with water three times for 1 min. Negatively charged (POD−PSS)$_c$ and positively charged PAH were then alternately adsorbed using the same procedure. Cyclic adsorption of (POD−PSS)$_c$ and PAH was conducted until the desired number of layers was deposited. All layers were assembled at 4 °C and maintained at this temperature throughout.

Quartz Crystal Microbalance (QCM) Measurements. QCM measurements were made by using a Q-sense D300 device equipped with a flow cell (Q-Sense AB, Västra Frölundra, Sweden). The temperature of the measurement chamber was kept at 20.5 °C during the experiments. A gold-coated 5 MHz AT-cut quartz crystal was excited at its third overtone (∼15 MHz) and the change in the resonance frequency (ΔF) was recorded. The frequency values obtained were divided by 3 for direct comparison with the base frequency data obtained at 5 MHz. The Sauerbrey equation was used to calculate the mass of the adsorbed layers from ΔF values.[28] For the setup employed, a correlation factor of $C = 17.7$ ng Hz^{-1} cm^{-2} applies.[29] The QCM electrodes were cleaned by piranha treatment, as described elsewhere.[30] A PEI layer was then deposited, followed by thoroughly rinsing with water. Alternating layers of PSS/POD or (POD−PSS)$_c$/PAH were then adsorbed onto the QCM electrodes, as described earlier.

Scanning Electron Microscopy (SEM). SEM images were recorded with a XL 30 FEG (Philips) instrument operated at an acceleration voltage of 2 kV. POD/PE tube samples were prepared by dissolving the PC membrane template from the coated membranes in dichloromethane, washing with water, and placing a drop of the diluted tube suspension onto a glass microscope slide (precleaned by ultrasonication in acetone for 10 min, ethanol rinsing, and nitrogen drying). The samples were sputter-coated with a thin gold film.

Transmission Electron Microscopy (TEM). TEM samples were prepared by placing a drop of the POD/PE tube suspension onto a TEM grid. A Philips CM 120 microscope operated at 120 kV was used for analysis.

UV−Visible Spectrophotometry. UV−vis spectra were recorded on a HP 8453 spectrophotometer (Agilent, Palo Alto, CA).

Enzymatic Activity Assays. A colorimetric assay was performed to determine the activity of POD immobilized in the films on the PC membranes. The test solution contained 7.5 mL of 0.21 mM *o*-dianisidine (0.05 M PB, pH 6.0), 0.1 mL of 30% (wt %) H_2O_2, and 2.4 mL of H_2O. The maximum UV absorption of the reaction product of *o*-dianisidine at 460 nm was used to determine the activity of POD in the sample.[20]

Results and Discussion

Multilayer Film Assembly. QCM experiments were first conducted to examine the formation of POD/PSS and (POD−

(21) Lvov, Y.; Caruso, F. *Anal. Chem.* **2001**, *73*, 4212.
(22) Wang, Y.; Caruso, F. *Adv. Funct. Mater.* **2004**, *14*, 1012.
(23) Cassagneau, T.; Caruso, F. *Adv. Mater.* **2002**, *14*, 1837.
(24) Liang, Z.; Susha, A. S.; Yu, A.; Caruso, F. *Adv. Mater.* **2003**, *15*, 1849.
(25) Ai, S.; Lu, G.; He, Q.; Li, J. *J. Am. Chem. Soc.* **2003**, *125*, 11140.
(26) Hou, S.; Harrell, C.; Trofin, L.; Kohli, P.; Martin, C. R. *J. Am. Chem. Soc.* **2004**, *126*, 5674.
(27) Data on the PC membrane properties can be found at http://www.millipore.com/catalogue.nsf/docs/C153.
(28) Sauerbrey, G. *Z. Phys.* **1959**, *155*, 206.
(29) Instrument Documentation D300, Q-Sense AB, Västra Frölunda, Sweden 2003.
(30) (a) Yu, A.; Caruso, F. *Anal. Chem.* **2003**, *75*, 3031. (b) Schütz, P.; Caruso, F. *Adv. Funct. Mater.* **2003**, *13*, 929.

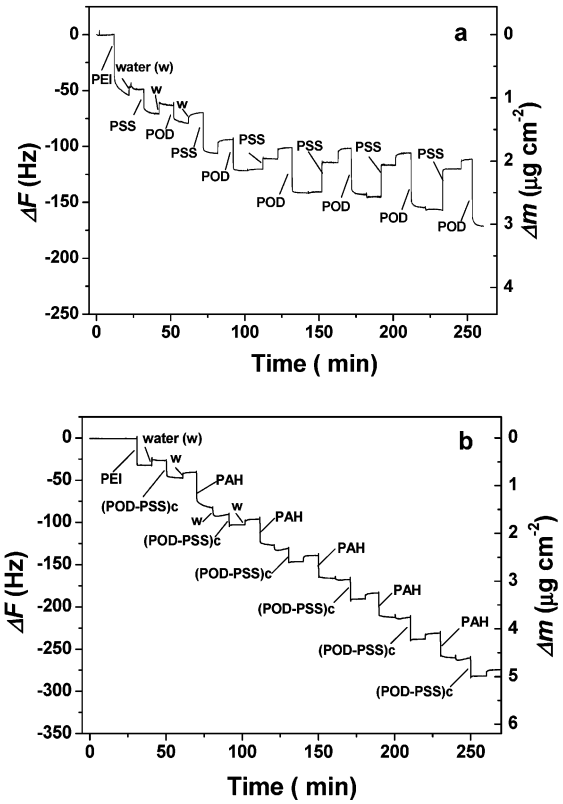

Figure 1. Real-time monitoring of the formation of POD/PSS (a) and $(POD-PSS)_c$/PAH (b) multilayer films on QCM electrodes. A PEI layer was deposited first, followed by alternating layers of POD (1 mg mL^{-1}, pH 5.0 PB) and PSS (1 mg mL^{-1}, 0.5 M NaCl) (a) or $(POD-PSS)_c$ (1 mg mL^{-1} POD/2 mg mL^{-1} PSS, pH 5.0 PB) and PAH (1 mg mL^{-1} containing 0.5 M NaCl) (b). Intermediate water washing steps were used.

$PSS)_c$/PAH multilayer films on planar supports. Figure 1 shows the ΔF and Δm trends for the formation of POD/PSS (a) and $(POD-PSS)_c$/PAH (b) multilayer films. The electrode was first primed with a layer of PEI, and alternating layers were then deposited with intermediate washing steps. The frequency decrease corresponds to an increase in adsorbed mass on the electrode, while the frequency increase during the washing steps is ascribed to the effect of ion concentration on the frequency in the setup used.[30b] Figure 1a shows QCM frequency decreases for the first two adsorption cycles of PSS and POD. However, subsequent adsorption steps yield frequency decreases for the POD adsorption steps and frequency increases for the PSS deposition steps, indicating that the films do not grow regularly. This is attributed to the stripping of POD from the surface upon exposure to PSS solutions and the formation of water-soluble POD−PSS complexes.[20] Similar results were reported earlier for the desorption of urease by poly(diallyldimethylammonium chloride) (PDDA) via the LbL method.[21] In that work it was shown that improved stability with respect to protein retention against polyelectrolyte stripping can be achieved by an additional nanoparticle layer (e.g., gold, silica, or magnetite nanoparticle) prior to adsorbing the enzyme.[21] Alternatively, the stability of enzymes in thin films can be significantly improved by adsorbing the enzyme in the form of a complex with an oppositely charged polyelectrolyte.[12,20] The formation of enzyme−polyelectrolyte complexes in solution has been extensively studied by several research groups.[31−33] Herein, we apply this latter approach to avoid

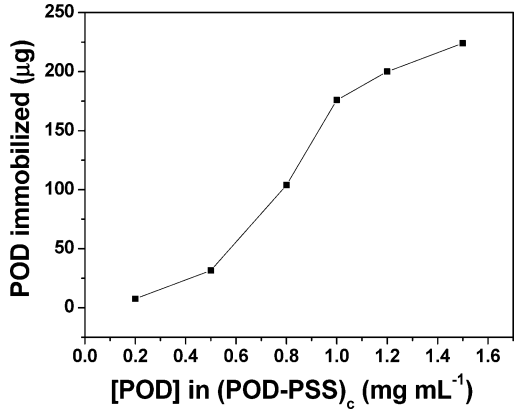

Figure 2. Plot of the POD concentration in the $(POD-PSS)_c$ solution versus the amount of POD adsorbed on PEI-modified PC membranes with pore diameters of 400 nm. The concentration ratio of POD/PSS in $(POD-PSS)_c$ was 1:2 (w/w), and the adsorption time was 60 min. The line drawn is to guide the eye.

enzyme loss from the surface in the LbL buildup of the enzyme/PE multilayer films on the porous membranes. We complexed POD (isoelectric point of 8.0) with PSS at pH 5.0 at a ratio of 1:2 w/w (POD/PSS), as this yields $(POD-PSS)_c$ that are negatively charged (ζ-potentials of ca. −50 mV are observed for $(POD-PSS)_c$-coated particles[20]). Figure 1b shows the in situ formation of $(POD-PSS)_c$/PAH multilayer films by alternately adsorbing $(POD-PSS)_c$ and PAH, with intermediate washing steps. A systematic decrease in the QCM frequency is observed for the $(POD-PSS)_c$/PAH deposition steps, indicating the successful formation of POD/PE multilayer films. The ΔF per $(POD-PSS)_c$/PAH bilayer is -43 ± 3 Hz. Using this ΔF value in the Sauerbrey relation,[29] a Δm of 761 ± 53 ng cm^{-2} is calculated. For comparison, a close-packed monomolecular layer of POD is expected to yield a Δm of ca. 350 ng cm^{-2}. It is noted that in the QCM measurements, the total oscillating mass is detected, and therefore any water hydrodynamically coupled to the films will contribute to the observed frequency change.

$(POD-PSS)_c$/PAH layers were then deposited onto PC membranes by using the same conditions as those employed for the QCM experiments, with the exception that sonication was applied for 2 min at the beginning of each adsorption step to aid transportation of the coating materials into the membrane pores. The amount of POD immobilized onto a PC membrane after the $(POD-PSS)_c$ adsorption step was determined by monitoring the difference in the absorbance of the $(POD-PSS)_c$ solution at 403 nm before and after exposure to the membrane. The POD absorption peak at 403 nm corresponds to the Soret absorption band of the iron (III) heme structure.[34] Figure 2 shows the influence of the $(POD-PSS)_c$ solution concentration (the ratio of POD/PSS was fixed at 1:2 w/w) on the quantity of POD immobilized on the 400-nm-pore PC membranes. For an adsorption time of 60 min,

(31) Margolin, A. L.; Sherstyuk, S. F.; Izumrudove, V. A.; Zezin, A. B.; Kabanov, V. A. *Eur. J. Biochem.* **1985**, *146*, 625.
(32) Zezin, A. B.; Izumrudov, V. A.; Kabanov, V. A. *Makromol. Chem., Macromol. Symp.* **1989**, *26*, 249.
(33) Izumi, T.; Hirata, M.; Takahashi, K.; Kokufuta, E. *J. Macromol. Sci., Pure Appl. Chem.* **1994**, *A31*, 39.
(34) (a) Theorell, H.; Ehrenberg, A. *Acta Chem. Scand.* **1951**, *5*, 823. (b) George, P.; Hanania, G. *Biochem. J.* **1953**, *55*, 236. (c) Nassar, A.-E. F.; Willis, W. S.; Rusling, J. F. *Anal. Chem.* **1995**, *67*, 2386.

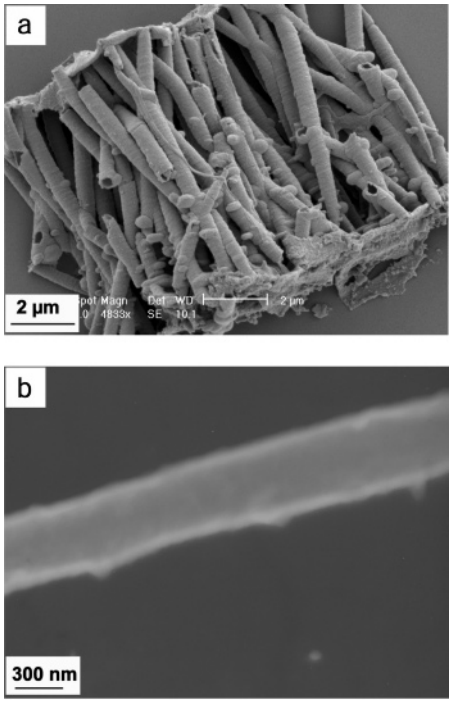

Figure 3. SEM (a) and TEM (b) images of POD/PE tubes obtained from 400-nm pore PC membranes coated with $[(POD-PSS)_c/PAH]_{20}$ multilayer films. The PC membrane was dissolved in dichloromethane. Solution compositions: $(POD-PSS)_c$ (1 mg mL^{-1} POD/2 mg mL^{-1} PSS, pH 5.0 PB); PAH (1 mg mL^{-1} containing 0.5 M NaCl).

the amount of POD immobilized on the membrane increases sharply with increasing POD concentration in the range 0.5−1.0 mg mL^{-1}. At a POD concentration of 0.5 mg mL^{-1}, the amount of immobilized POD is 32 μg. This value increases 5-fold to 176 μg at a POD concentration of 1.0 mg mL^{-1}. However, above this point, a 50% further increase in the POD concentration yields only a 28% increase in adsorbed POD. For our coating experiments, we chose to employ solutions containing 1.0 mg mL^{-1} POD and 2.0 mg mL^{-1} PSS.

Multilayer Film Characterization. The $(POD-PSS)_c$/PAH multilayers deposited on PC porous templates were characterized by SEM and TEM after dissolving the PC membrane template. Figure 3a shows an SEM image of $[(POD-PSS)_c/PAH)]_{20}$ multilayers formed on PC membranes with 400-nm-diameter pores and subsequently released from the membrane. Tubular structures of various lengths can be seen. Few tubes of length of ca. 10 μm, corresponding to the thickness of the membrane, are observed. The formation of shorter tubes reflects the fact that some cylindrical pores in the PC membranes are not continuous throughout the entire thickness of the membrane. Additionally, tube breakage during sample preparation (template dissolution, sonication, and drying) may also be a contributing factor. The SEM image also shows the POD/PE coating resulting from adsorption on the top and bottom surfaces of the membrane. TEM analysis of the same sample further confirms the tubular structure (Figure 3b). As calculated from TEM, the outer diameters of the tubes are approximately 400 nm, corresponding to the pore diameter of the membrane used. The wall thickness of the tube with 20 bilayers is 90 ± 8 nm, or 4−5 nm/bilayer. (One bilayer corresponds to the adsorption of a layer of $(POD-PSS)_c$ and another of PAH.) This value is close to the wall thickness expected by assuming a thickness of ∼1 nm per PE layer,[35] and that POD forms a monolayer (ca. 3.5 nm[13,20]). Tubes with thicknesses less than 50 nm (i.e., tubes comprising less than 10 bilayers) showed collapsed structures (as observed by SEM), in accordance with our previous work on PE tubes.[24] We also deposited POD/PE multilayer films on PC membranes with 100-nm-diameter pores. Tube structures similar to those shown in Figure 3 but with diameters of ∼100 nm were obtained (data not shown).

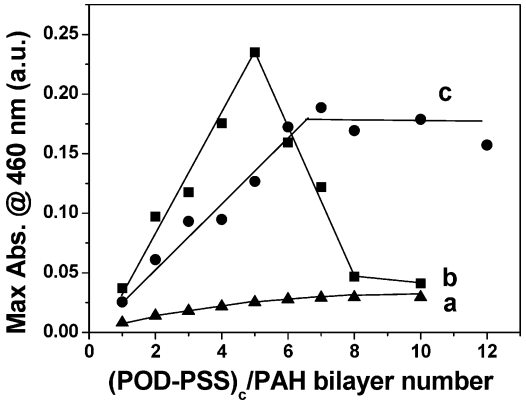

Figure 4. Film enzymatic activity (absorption of product of *o*-dianisidine at 460 nm) as a function of bilayer number for $(POD-PSS)_c$/PAH multilayers deposited on quartz slides (a) and PC membranes with 100-nm (b) or 400-nm (c) pores. Solution compositions: $(POD-PSS)_c$ (1 mg mL^{-1} POD/2 mg mL^{-1} PSS, pH 5.0 PB) and PAH (1 mg mL^{-1} containing 0.5 M NaCl). The lines drawn are to guide the eye. The activity data for the films on the quartz slides were normalized to the same geometrical area of the PC membranes.

POD Activity Assay. A colorimetric assay based on the reaction of *o*-dianisidine and H_2O_2 was used for measuring the activity of membrane-immobilized POD.[20] The reaction product of *o*-dianisidine has an absorption peak at 460 nm, which can be used to determine the total enzymatic activity of the film. Figure 4 (curve b) shows the total activity of a POD/PE-coated membrane (with 100-nm pores) as a function of the number of $(POD-PSS)_c$/PAH bilayers deposited. First, the total POD activity of the membrane increases with increasing POD content in the film. The maximum membrane activity is obtained for five $(POD-PSS)_c$/PAH bilayers, after which the total enzymatic activity begins to decrease, finally plateauing after eight bilayers. Considering that the multilayer films also deposit on the top and bottom surfaces of the membrane (see Figure 3a), we attribute the sharp activity decrease to increased blockage of the membrane pores. Pore blockage would manifest itself as an activity decrease because of substrate diffusion limitations and reduced enzyme accessibility.[1,12,19,20] To examine this further, we deposited $(POD-PSS)_c$/PAH multilayer films on nonporous substrates (quartz slides). As shown in Figure 4 (curve a), the activity of the enzyme films constructed on the quartz slides increases up to seven bilayers. The deposition of further enzyme−PE layers does not yield increased activity, which is again due to substrate diffusion limitations upon increasing the film thickness. The activity

(35) Caruso, F.; Lichtenfeld, H.; Donath, E.; Möhwald, H. *Macromolecules* **1999**, *32*, 2317.

saturation value obtained (0.03) is close to the corresponding values measured for the 100-nm pore diameter membranes (0.04, curve b), supporting the argument of pore blockage.

The point at which pore closure becomes dominant is dependent upon the pore diameter of the membranes. As shown in Figure 4 (curve c), $(POD-PSS)_c$/PAH multilayer films deposited onto PC membranes with 400-nm pores display qualitative trends in activity similar to those of identical films deposited on quartz slides (curve a). No sharp activity decrease is seen, even for membranes coated with 12 bilayers.

The approximate surface area of the membranes was calculated by an analysis of the number of pores and pore diameter of the membranes (assuming the pores extend throughout the membrane). Using this method, membranes with 100-nm pores (∼4% porosity) have a surface area of ca. 298 cm^2, while the surface area for the membranes with 400-nm pores (∼13% porosity) is ca. 235 cm^2. These values are approximately 9 and 7 times larger, respectively, than that of a nonporous substrate with the same geometrical area (i.e., 33.2 cm^2). Notably, the relative difference in the surface area values is in good agreement with the experimental activity data obtained. Compared with the same enzyme multilayer films constructed on quartz slides (Figure 4 (curve a)), the maximum total membrane activity values are 9 times larger for the 100-nm diameter pore membranes (Figure 4 (curve b), bilayer number = 5) and 7 times larger for the 400-nm pore diameter membranes (Figure 4 (curve c), bilayer number = 7).

In summary, we have demonstrated that enzyme-modified PC porous membranes with tailored bioactivity can be prepared by the alternate deposition of $(POD-PSS)_c$ and oppositely charged PAH. The film bioactivity is related to the total surface area of the membrane, which is governed by the pore size and porosity, and the number of enzyme-containing layers deposited. Activity values up to approximately 9-fold higher are obtained for POD/PE-modified membranes than for the same films deposited onto (nonporous) quartz slides. By judicious selection of membrane templates with higher porosity (e.g., 40−50% for alumina membranes), much higher activities (>1 order of magnitude) should be attainable. Due to the flexibility of the LbL technique, the current work provides a facile approach to prepare high-surface-area supported enzyme films with diverse composition, structure, and bioactivity.

Acknowledgment. J. Quinn is thanked for assistance with the SEM measurements, and K. Katagiri and Y. Wang are thanked for TEM measurements. Y. Wang and B. Radt are acknowledged for helpful discussions. This work was supported by the Australian Research Council under the Federation Fellowship and Discovery Project schemes, and the Victorian STI Initiative.

CM048659H